

Article

A Peptoid with Extended Shape in Water

Jumpei Morimoto, Yasuhiro Fukuda, Daisuke Kuroda, Takumu Watanabe, Fumihiko Yoshida, Mizue Asada, Toshikazu Nakamura, Akinobu Senoo, Satoru Nagatoishi, Kouhei Tsumoto, and Shinsuke Sando

J. Am. Chem. Soc., **Just Accepted Manuscript** • DOI: 10.1021/jacs.9b04371 • Publication Date (Web): 12 Aug 2019

Downloaded from pubs.acs.org on August 13, 2019

Just Accepted

“Just Accepted” manuscripts have been peer-reviewed and accepted for publication. They are posted online prior to technical editing, formatting for publication and author proofing. The American Chemical Society provides “Just Accepted” as a service to the research community to expedite the dissemination of scientific material as soon as possible after acceptance. “Just Accepted” manuscripts appear in full in PDF format accompanied by an HTML abstract. “Just Accepted” manuscripts have been fully peer reviewed, but should not be considered the official version of record. They are citable by the Digital Object Identifier (DOI®). “Just Accepted” is an optional service offered to authors. Therefore, the “Just Accepted” Web site may not include all articles that will be published in the journal. After a manuscript is technically edited and formatted, it will be removed from the “Just Accepted” Web site and published as an ASAP article. Note that technical editing may introduce minor changes to the manuscript text and/or graphics which could affect content, and all legal disclaimers and ethical guidelines that apply to the journal pertain. ACS cannot be held responsible for errors or consequences arising from the use of information contained in these “Just Accepted” manuscripts.

A Peptoid with Extended Shape in Water

Jumpei Morimoto,^{†,‡,*} Yasuhiro Fukuda,^{†,‡} Daisuke Kuroda,^{†,§} Takumu Watanabe,[†] Fumihiko Yoshida,[†] Mizue Asada,[¶] Toshikazu Nakamura,[¶] Akinobu Senoo,[†] Satoru Nagatoishi,^{†,§,||} Kouhei Tsumoto,^{†,§,||} and Shinsuke Sando^{†,§,*}

[†]Department of Chemistry and Biotechnology, Graduate School of Engineering, The University of Tokyo, 7-3-1 Hongo, Bunkyo-ku, Tokyo 113-8656, Japan.

[§]Department of Bioengineering, Graduate School of Engineering, The University of Tokyo, 7-3-1 Hongo, Bunkyo-ku, Tokyo 113-8656, Japan.

[¶]Department of Materials Molecular Science, Institute for Molecular Science, 38 Nishigo-naka, Myodaiji, Okazaki 444-8585, Japan.

^{||}Institute of Medical Science, The University of Tokyo, 4-6-1 Shirokanedai, Minato-ku, Tokyo, 108-8639, Japan.

ABSTRACT: The term “peptoids” was introduced decades ago to describe peptide analogs that exhibit better physicochemical and pharmacokinetic properties than peptides. Oligo(*N*-substituted glycine) (oligo-NSG) was previously proposed as a peptoid due to its high proteolytic resistance and membrane permeability. However, oligo-NSG is conformationally flexible and ensuring a defined shape in water is difficult. This conformational flexibility severely limits the biological application of oligo-NSG. Here, we propose oligo(*N*-substituted alanine) (oligo-NSA) as a peptoid that forms a defined shape in water. The synthetic method established in this study enabled the first isolation and conformational study of optically pure oligo-NSA. Computational simulations, crystallographic studies and spectroscopic analysis demonstrated the well-defined extended shape of oligo-NSA realized by backbone steric effects. This new class of peptoid achieves the constrained conformation without any assistance of *N*-substituents and serves as a scaffold for displaying functional groups in well-defined three-dimensional space in water, which leads to effective biomolecular recognition.

INTRODUCTION

Peptidomimetic synthetic oligoamides with better physicochemical and pharmacokinetic properties than peptides have been long sought and many examples of such oligomers have been reported, e.g. β -peptides,^{1,2} oligomers of α -aminoisobutyric acids,^{3,4} and oligoureas.^{5,6} Oligo(*N*-substituted glycine) (oligo-NSG) was proposed as one such oligoamide and called “peptoid”^{7,8} in 1992.⁹ Oligo-NSG is a rare example of synthetic oligomers that combines high proteolytic resistance¹⁰ and high membrane permeability¹¹ derived from its *N*-substituted amide backbone. In addition, submonomer synthetic methods of oligo-NSG allow the introduction of a diverse set of proteinogenic and nonproteinogenic functional groups as *N*-substituents.¹² These important unique features of oligo-NSG are advantageous over other peptidomimetic oligoamides for generating drug candidates. However, the backbone of the NSG-type peptoid is intrinsically flexible; therefore, a peptoid that exhibits high affinity to biomolecules has not been reported except for rare exceptions.¹³ To overcome this limitation, extensive research studies have constrained the conformation of oligo-NSG using elaborate *N*-substituents. These efforts successfully realized oligo-NSGs with defined shapes in organic solvents, such as helices similar to polyproline type I and type II helices.¹⁴⁻²² However, such conformational regulation generally requires introduction of multiple bulky hydrophobic *N*-substituents that severely

compromise water solubility and/or restrict the choice of *N*-substituents. The introduction of charged groups is effective to compensate the water solubility of these peptoids,²³⁻²⁶ but these restrictions reduce the design flexibility of oligo-NSGs. After the pioneering works by Zuckermann and coworkers on oligo-NSGs, “peptoids” has been recognized as the term describing oligo-(*N*-substituted amides) and many other peptoids have been developed, e.g. β -peptoids,²⁷⁻³⁰ hydrazinoazapeptoids,³¹ aminoxy peptoids,³² and arylopeptoids.^{33,34} However, for these oligomers also, it is difficult to achieve conformationally constrained oligomers with good water solubility.

The introduction of methyl substituents on the backbone α -carbon of oligo-NSG to make oligo(*N*-substituted alanine) (oligo-NSA) (Figure 1a) was previously proposed by Kodadek and coworkers to constrain the conformation of peptoids via the local steric effects on the backbone.^{35,36} The constrained conformation was reasoned from an analogy of *N*-methylated peptides. More specifically, the introduced methyl substituent would produce steric repulsion, known as pseudo-1,3-allylic strain,^{37,38} with the carbonyl oxygen of the preceding residue and the *N*-substituent of the following residue and restrict rotation about the ϕ and ψ angles (Figure 1b). Moreover, steric repulsion between two methyl substituents on neighboring residues would destabilize the *cis* conformation of the intervening amide bond and bias the amide bond to *trans*, i.e.

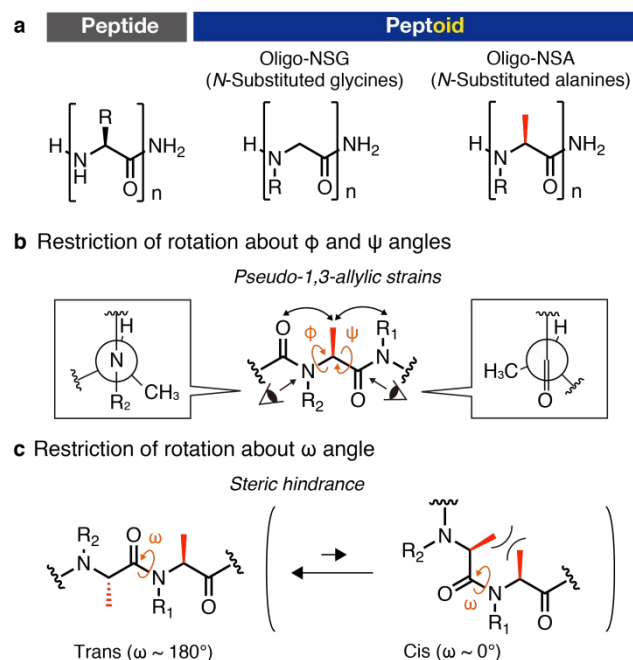


Figure 1. Chemical structure and proposed conformational regulation by steric effects of oligo-NSA. (a) Chemical structures of peptide and peptoid. (b) The bond rotations about ϕ and ψ angles of oligo-NSA are restricted due to the pseudo-1,3-allylic strains. (c) ω angle of oligo-NSA is biased to $\sim 180^\circ$ due to the steric repulsion between backbone structures.

the ω angles are restricted to the value around 180° (Figure 1c). Because it does not require introduction of bulky *N*-substituents, but requires the introduction of only a small methyl substituent, this strategy is suitable for realizing a peptoid that forms a defined shape in biological environment and displays various functional groups as *N*-substituents into well-defined three-dimensional spaces in water. Despite the potential utility of oligo-NSA, optically pure oligo-NSAs possessing *N*-substituents other than methyl have not been reported because of the synthetic difficulty of such oligomers. Thus, the validity of the constrained conformation of oligo-NSA remains to be examined and establishment of synthetic scheme for such a useful oligomer has been awaited.

Here, we established a synthetic method for oligo-NSA and isolated optically pure oligo-NSAs bearing *N*-substituents larger than methyl for the first time. Using the synthesized oligo-NSAs, conformational studies of oligo-NSAs were conducted and the studies revealed that oligo-NSA achieves a defined shape in water and serves as a scaffold of an extended shape displaying functional groups in a well-defined three-dimensional space in water. The well-defined extended shape of oligo-NSA was utilized to rationally generate a protein ligand, which demonstrated the utility of this new peptoid for biological applications.

RESULTS AND DISCUSSION

Quantum mechanical studies. First, we performed computational simulations to predict how the pseudo-1,3-allylic strain would constrain the conformation of peptoid and what the conformation of oligo-NSA would look like. Minimal components of oligo-NSG, i.e. acetyl-*N*-methylglycine dimethylamide, and oligo-NSA, i.e. acetyl-*N*-methylalanine

dimethylamide, were subjected to quantum mechanical (QM) calculations to generate Ramachandran-type energy diagrams over ϕ and ψ angles. The diagram of oligo-NSG had a relatively large region within 10 kcal/mol from the lowest energy point (Figure 2a), which is consistent with the previous reports of similar calculations.^{39,40} In contrast, the diagram of oligo-NSA had a narrow region with the lowest energy at around $(\phi, \psi) = (-120^\circ, 90^\circ)$ and the surrounding region was predominantly favored over other regions (Figure 2b). To understand how the *N*-substituents will be oriented on oligo-NSA, we have also examined the preferred χ angles of acetyl-*N*-ethylalanine dimethylamide with fixed ϕ and ψ angles of the lowest energy point; $(\phi, \psi) = (-120^\circ, 90^\circ)$. As a result, 100° and -100° were determined to be the χ angles of the lowest energy (Figure S1). Based on this χ scan, energy diagrams of NSA over ϕ and ψ angles were re-examined using the χ angles of 100° and -100° for acetyl-*N*-ethylalanine dimethylamide as a minimal model of oligo-NSA with *N*-substituents larger than methyl. For the χ angle of 100° , the lowest energy angles were slightly shifted and became $(\phi, \psi) = (-105^\circ, 105^\circ)$, but, overall for both χ angles, the allowed region was similar to the above-mentioned landscape of acetyl-*N*-methylalanine dimethylamide (Figure 2c and d), which suggests that the structure of *N*-substituent does not largely affect the backbone conformation. These results support the hypothesis that introduction of a methyl substituent on the α -carbon of NSG would locally restrict the bond rotations about all the backbone dihedral angles. (For the definition of each dihedral angle, see Figure 2g and h.)

Based on the QM calculation of the monomeric NSA structure, we generated model structures of oligo-NSA. The models were built using dihedral angles (χ, ϕ, ψ, ω) of either $(100^\circ, -105^\circ, 105^\circ, 180^\circ)$ or $(-100^\circ, -120^\circ, 90^\circ, 180^\circ)$ and optimized with QM calculations using an implicit water model (Figure 2e and f). With either set of dihedral angles, the optimized structure of the oligo-NSA resulted in an extended shape. The conformation with χ angle of -100° was 1.4 kcal/mol more stable than the conformation with χ angle of 100° , indicating that the χ angle forms -100° a little more preferably in an oligomer. The extended shape of oligo-NSA is realized by the iterative regulation of backbone dihedral angles driven by the steric effects. This backbone-dictated shape would be useful as a scaffold for biomolecular recognition because the backbone forms a constrained conformation *N*-substituent-independently and functional groups introduced as *N*-substituents would be displayed in well-dispersed space without causing intramolecular association of hydrophobic residues.

Synthesis. To experimentally validate the extended conformation of oligo-NSA, optically pure oligomers must be isolated in multimilligram quantities. Although peptides or oligo-NSGs with nonconsecutive NSA residues have been reported,^{35,41–44} there have been no reports for oligomers with consecutive NSA residues with *N*-substituents other than methyl. The extended shape of oligo-NSA would be realized only by such oligomers with consecutive NSA residues. Therefore, we first established a synthetic method for optically pure oligo-NSAs. The most promising synthetic method was the submonomer synthetic method using chiral 2-bromopropionic acid and primary amine (Figure S2a) proposed by Zuckerman and Kodadek^{35,45} because this method

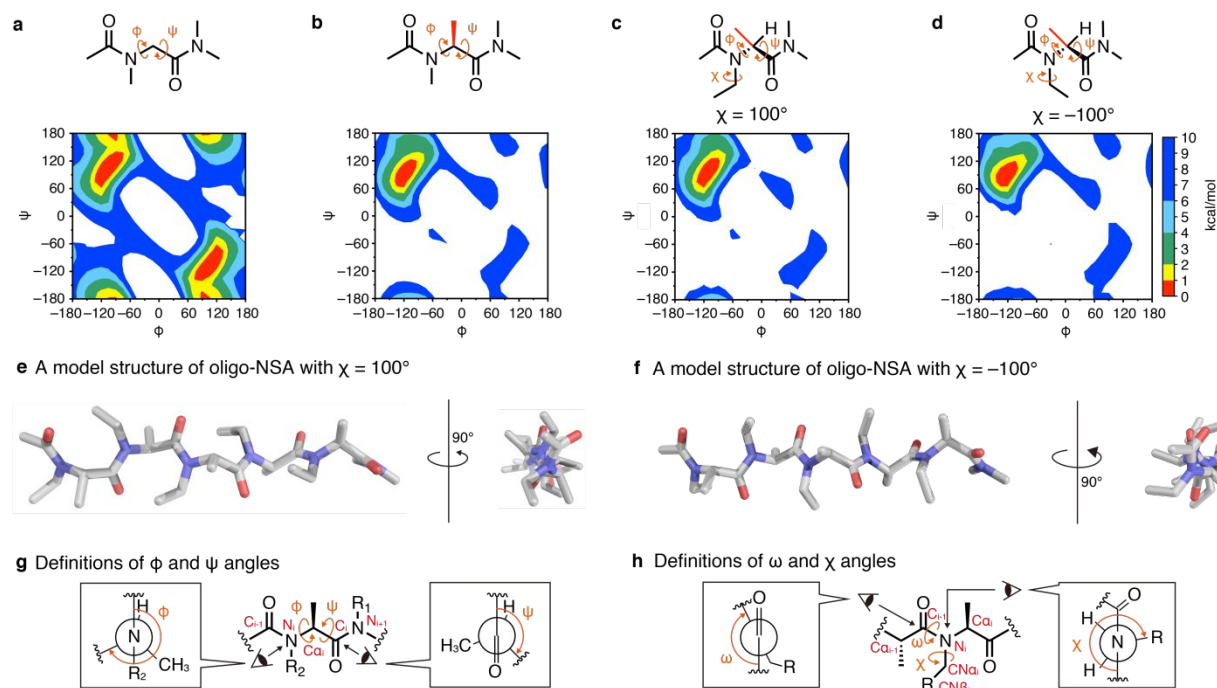


Figure 2. (a) An energy diagram of acetyl-*N*-methylglycine dimethylamide as a minimal model of oligo-NSG. (b) An energy diagram of acetyl-*N*-methylalanine dimethylamide as a minimal model of oligo-NSA. (c, d) An energy diagram of acetyl-*N*-ethylalanine dimethylamide as a minimal model of oligo-NSA with *N*-substituents larger than methyl. The χ angle was fixed to 100° for c and -100° for d based on the results of χ scan (Figure S1). For these diagrams, regions that have energies above 10 kcal/mol from the lowest energy point were colored in white. (e) A model structure of acetyl-*N*-ethylalanine pentamer that was optimized from an initial conformation of $(\chi, \phi, \psi, \omega) = (100^\circ, -105^\circ, 105^\circ, 180^\circ)$ with a QM calculation. (f) A model structure of acetyl-*N*-ethylalanine pentamer that was optimized from an initial conformation of $(\chi, \phi, \psi, \omega) = (-100^\circ, -120^\circ, 90^\circ, 180^\circ)$ with a QM calculation. (g) Definitions of ϕ angle ($C_{i-1}, N_i, C\alpha_i, C_i$) and ψ angle ($N_i, C\alpha_i, C_i, N_{i+1}$) of oligo-NSA. (h) Definitions of ω angle ($C\alpha_{i-1}, C_{i-1}, N_i, C\alpha_i$) and χ angle ($C\alpha_i, N_i, CN\alpha_i, CN\beta_i$) of oligo-NSA.

does not require prior preparation of individual *N*-substituted alanines, but only requires commercially available simple submonomers. However, due to the racemization prone nature of 2-bromopropionic acid,⁴⁶ efficient synthesis of optically pure oligo-NSAs using the method was unsuccessful (Figure S2b–d). Therefore, we turned to another synthetic method for oligo-NSAs reported by Pels and Kodadek that utilizes Fmoc-alanine and aldehydes as submonomers⁴² (Figure S3a). This method also only requires commercially available submonomers, which is equally attractive to the abovementioned submonomer synthetic method. However, in their report, consecutive introduction of NSA residues was avoided due to the inefficient coupling reaction of Fmoc-alanine on *N*-substituted alanine terminus. Therefore, we investigated various coupling conditions for Fmoc-alanine on *N*-substituted alanine terminus to achieve introduction of consecutive NSA residues (Figure S3b). Among the tested conditions, coupling reaction using 1-ethoxycarbonyl-2-ethoxy-1,2-dihydroquinoline (EEDQ) in dioxane gave the highest coupling yield (Figure S3c and Figure S4). Double coupling at 60°C for 3 h each or at 100°C by microwave heating for 1 h each using EEDQ gave a quantitative conversion with no detectable amount of racemization (Figure S3c and d). Encouraged by the quantitative conversion for the challenging acylation reaction, 1–5 mer of NSAs were synthesized on resin using the optimized conditions (Figure 3a). Note that a trityl linker was recruited to allow cleavage of the synthesized oligomers from resin with a mild acidic condition (30% hexafluoroisopropanol in dichloromethane)

due to the highly acid labile nature of NSAs^{47,48} and a piperazine spacer was inserted between the trityl linker and NSA oligomers to prevent diketopiperazine formation during synthesis. All 1–5 mer of NSAs were obtained with decent yields (Figures 3b and S5–8). There have been reports about oligo-NSGs containing skipped NSA residues,^{35,42–44,49–51} but this is the first report of the isolation of optically pure oligo-NSAs containing consecutive NSA residues with *N*-substituents other than methyl.

To demonstrate that polar residues can be also introduced on oligo-NSA, we synthesized heterooligomers containing amine and carboxylic acid on *N*-substituents. We synthesized pentamers with either Boc/tBu-protected amine/carboxylic acid (**S6**) or Alloc/Allyl-protected amine/carboxylic acid (**S7**) (Figure S9a and b). Although the yields were low (1% and 3%, respectively), both the pentamers were successfully synthesized and isolated. Deprotection of Alloc/Allyl groups of **S7** on resin successfully led to isolation of a pentamer with free amine and carboxylic acid on *N*-substituents (**S8**). (Figure S9c)

It should be noted that even the longest oligo-NSA **5** with no polar *N*-substituents exhibited good water solubility. Oligo-NSA **5** was soluble in water up to 270 mM (Figure S10). As a control, an oligo-NSG with the same chain length and the same *N*-substituents (**5-NSG**) was synthesized and its water solubility was evaluated. The oligomer was soluble up to 320 mM, which is not significantly different from that of oligo-NSA. This validates our strategy that the introduction of methyl substituents on backbone carbons constrains the

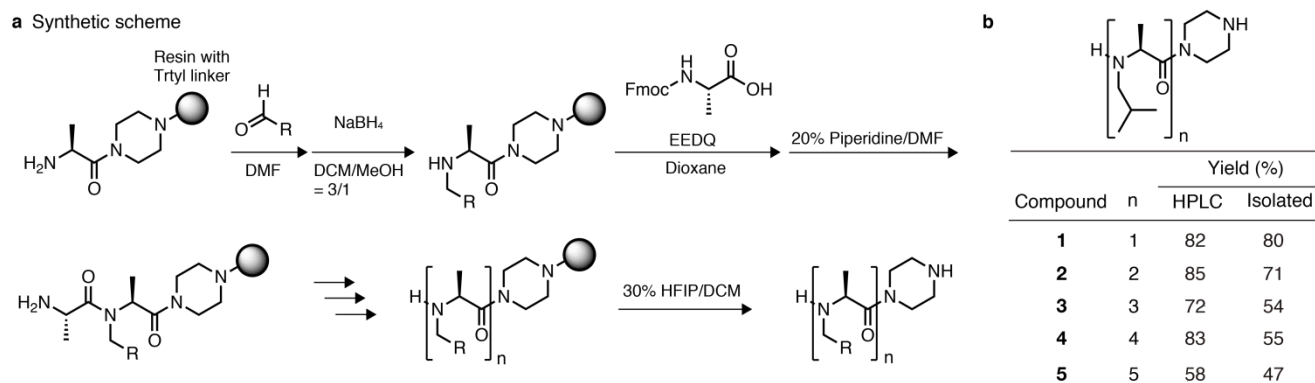


Figure 3. Submonomeric synthesis of oligo-NSA using Fmoc-Ala-OH and aldehyde. (a) Synthetic scheme of oligo-NSA. Resin with a trityl linker was utilized to allow cleavage of the synthesized compounds from resin using mild acidic conditions. The piperazine spacer was introduced between the trityl linker and oligo-NSAs to prevent diketopiperazine formation during synthesis. (b) Yields of *N*-isobutylalanine 1–5 mer (**1–5**). HPLC chromatograms of crude and purified products are listed on Figures S5 and S6. For monomer (**1**), ¹H and ¹³C NMR spectra are shown on Figures S7 and S8.

conformation of peptoids without reducing their water solubility. As a piperazine group was previously shown to improve the water solubility of oligo-NSG,²⁶ the oligo-NSA without the terminal piperazine group (**5-amide**) was also synthesized to investigate the influence of the terminal group on water solubility. As expected, this oligomer exhibited lower water solubility than the oligomer with a piperazine group, but the oligomer with a C-terminal amide was still soluble up to 87 mM. (Figure S11 shows the HPLC chromatograms of **5-NSG** and **5-amide** after purification.) These results demonstrated the utility of the oligo-NSA for biological applications.

X-ray crystallographic study and molecular dynamics simulations. With the optimized synthetic method, several oligo-NSAs were synthesized and X-ray crystallographic analysis was conducted to experimentally reveal a preferred conformation of oligo-NSAs. Among the various conditions tested for the synthesized oligomers, crystals of *N*-benzylalanine pentamer (Figure 4a, compound **6**) were grown via slow evaporation from a cosolvent of hexane and dichloromethane. The structure was solved by X-ray crystallographic analysis (Figures 4b and c, and S12). In the crystal, the oligomer exhibited an extended shape that is consistent with the predicted steric effects and QM calculations (Figure 4c). First, all the amide bonds were trans as expected from the steric repulsion of backbone structures. Second, pseudo-1,3-allylic strains were seen at all the ϕ and ψ angles and the dihedral angles of all the residues were consequently restricted to the region within 2 kcal/mol from the lowest energy point on the energy diagram generated by the QM calculations (Figure S13). To assess how the crystal structure relates to the above-described model structure, the crystal structure was overlaid with one of the model structures shown in Figure 2f that gave a lower energy than the other model structure shown in Figure 2e. Overall, the backbone conformation of the crystal structure and the model structure well overlapped with each other except for the *N*-terminal residue, which is inevitably different because the *N*-terminal amine of the crystallized oligomer is not acylated and does not experience pseudo-1,3-allylic strain (Figure 4d). The root-mean-square deviation (RMSD) of backbone atoms (N, C α , and carbonyl C) other than the *N*-terminal residues for the model and the crystal structures was 0.289 Å. As seen in the model structure and also in the crystal, all the *N*-substituents

were well separated on the oligomer and no obvious contacts with backbone or other *N*-substituents were observed, suggesting that the extended shape of oligo-NSA is dictated solely by backbone steric effects and independently from *N*-substituents. This makes the oligo-NSA a favorable scaffold for displaying functional groups into well-dispersed three-dimensional space without causing intramolecular association of hydrophobic residues. *N*-substituents on every other residue are displayed in the same directions. The distance from one residue to the one after the next is 6.5–7.0 Å in the crystal. *N*-methylated peptides were also previously reported to exhibit similar side chain orientations with similar intervals in crystals.⁵² This is reasonable considering the same pseudo-1,3-allylic strains are the determining factors of the constrained conformations of these two oligomers. It is notable that the relative arrangements of side chains from backbones differ for these two oligomers, which may lead to different types of applications for each oligomer. Furthermore, a combination of these two types of oligomers may expand their future utility.

To obtain insights into how much the conformation of oligo-NSA observed in the crystal is stable in aqueous solution, molecular dynamics (MD) calculations of the *N*-benzylalanine pentamer were conducted using the crystal structure as the initial conformation with explicit solvent. The accuracy of computational simulations depends on the physical models of interactions. MD simulations of peptoids have been conducted based on traditional protein force fields, which successfully reproduced some experimental observations, such as major conformations of NMR or X-ray crystal structures.^{53–55} Therefore, we exploited the CHARMM36m/CGenFF force field to assess the stability and dynamic behavior of oligo-NSAs in solution. The calculation was performed for 500 ns at 298 K with five trials using the TIP3P water model. As a result, the ϕ and ψ angles were in the region within 4 kcal/mol from the lowest energy point on the energy diagram generated from the QM calculations for 95% of the simulated time (Figure S14). The ω angles were also kept at around 180° for all the simulated time (Figure S15), although this does not necessarily support the stability of trans amide bond because the kinetics of trans/cis isomerization *N*-substituted amide is much slower than the simulated time.⁵⁶ Therefore, the ω angles must be also evaluated spectroscopically (see the NMR analysis below).

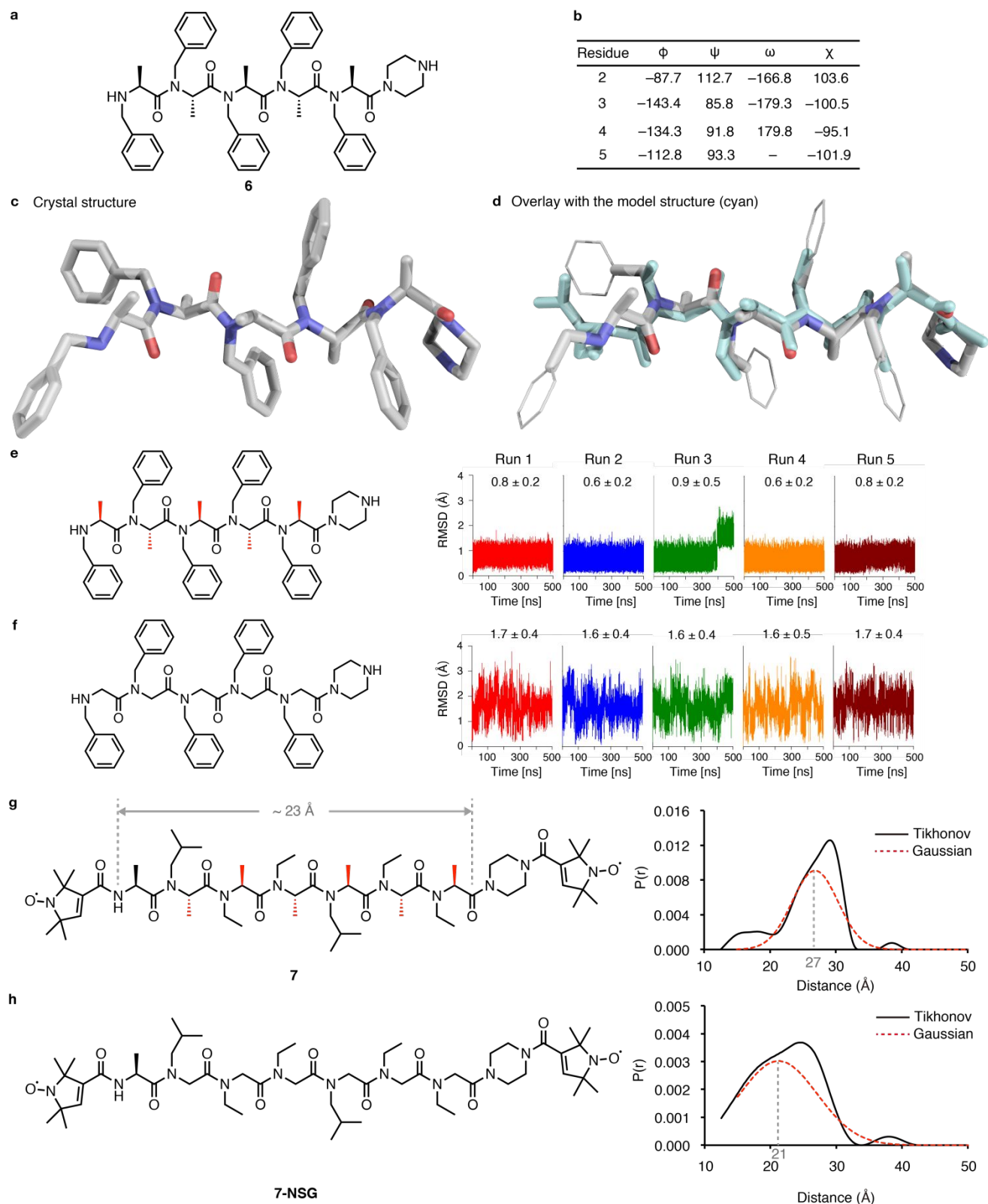


Figure 4. (a) Chemical structure of oligo-NSA **6** subjected to X-ray crystallographic analysis. (b) Dihedral angles of **6** observed in the crystal. (c) Crystal structure of **6**. (d) An overlay of the crystal structure and the model structure shown in Figure 2f (cyan). (e) RMSD value of the oligo-NSA **6** during each MD run. The average and standard deviations are shown above each plot. (f) RMSD value of the oligo-NSG during each MD runs. (g) Distribution of end-to-end distance of oligo-NSA (**7**) and (h) oligo-NSG (**7-NSG**) measured by DEER experiment. The distributions of distance between the two spins were calculated with Tikhonov regularization (solid black line) and Gaussian model fitting (dashed red line). The estimated length of oligo-NSA when it forms the predicted extended shape is labeled above the structure. The average length of the oligomer in the Gaussian model fitting is described in gray in the graph.

Because of the restricted rotations about these backbone dihedral angles, the oligomer well sustained an extended shape with a RMSD value of the α -carbons of the oligomer of only 0.5–0.9 Å on average, when compared to the initial crystal structure, for all the five runs (Figure 4e). As an exception, the RMSD value of the third run increased to ~ 2 Å at around 400 ns. The conformations observed during the last 100 ns of the third run were little bent from the initial extended conformation due to transitions of ϕ angles from around at -120° to around at 70° . However, the dihedral angles seen in the bent conformations correspond to a high-energy region on the Ramachandran-type plot (the upper-right blue region of Figure 2b); therefore, the conformations are presumably a minor population. In addition, the χ angles of the oligomers were also restricted to around -100° and 100° , which were calculated to be low in energy in the QM calculations (Figure S16). In contrast, when the same MD simulations were run for the oligomer of NSG backbone using the same backbone conformation as the initial structure of oligo-NSA, the ϕ and ψ angles of all the residues were distributed in much larger ranges (Figure S17) and the RMSD value was also much larger at 1.7 Å on average (Figure 4f). Interestingly, when an oligomer with alternate NSA and NSG residues were subjected to the same calculation, the dihedral angles of NSA residues were constrained but those of NSG residues were not constrained (Figure S18a), which led to distortion of the initial extended shape and a large conformational fluctuation (Figure S18b). This result agrees with the assumption that the extended shape is only realized by oligomers with consecutive NSA residues with no intervening NSG residues. This is consistent with the previous report that oligo-NSGs with alternate NSA residues are intrinsically disordered.⁴³

To confirm the validity of our MD simulations, we also performed both QM and molecular mechanics (MM) dihedral (ϕ , ψ) scanning, and described one-dimensional energy profiles as a function of each dihedral (Figure S19). The energy minima of the MM potential were in the close vicinity to those of the QM results, also corresponding to the dihedral angles observed in the crystal structure. These results imply that our simulations were able to capture the microscopic detail of the peptoid dynamics.

Although our computational results were in good agreement with the experimental results as described later, there is still room for improvement in describing molecular interactions. In addition to the continuing developments of protein force fields,⁵⁷ a new force field has been parameterized for an NSG peptoid based on experimental data (NMR and X-ray crystallography) and QM calculations.^{58,59} Likewise, our success of experimentally synthesizing oligo-NSAs and solving the crystal structure will also enable us to develop a new force field for oligo-NSA peptoids in future.

To complement our computational simulations and to experimentally validate the stability of the extended shape of oligo-NSA in water, we measured the end-to-end distance of oligo-NSA using electron paramagnetic resonance (EPR) spectroscopy. More specifically, we used the EPR-based method, i.e. a double electron–electron resonance (DEER/PELDOR) experiment.^{60–63} We synthesized an NSA hexamer (7) composed of ethyl and isobutyl *N*-substituents and labeled a nitroxide radical on both termini of the oligomer (Figure S20). A non-*N*-substituted alanine residue was inserted between the *N*-terminal label and the *N*-terminus of oligo-NSA to enhance the labeling reaction. Because the nitroxide spin

label is small and rigid in structure, the end-to-end distance was not largely affected by the labels. The oligomer in 1:1 H₂O/DMSO mixture was rapidly frozen at 20 K and subjected to the DEER measurement (Figures S21 and 22). This flash-freezing process is supposed to preserve the conformational distribution of peptides in solution at ambient temperature.⁶⁴ As a result, the mean distance of oligo-NSA determined from Gaussian fitting was 27 Å and the distance distribution was 5 Å (Figure 4g). In the model extended shape of oligo-NSA (Figure 2f), the distance between the two amide nitrogens of neighboring residues was 3.3 Å on average. Therefore, the NSA hexamer with an *N*-terminal alanine residue is expected to be ~ 23 Å in length when it forms the predicted extended structure. As a C-terminal piperazine spacer and two spin labels are appended to the oligomer, it is reasonable to consider that the observed 27 Å indicates that the oligo-NSA forms the predicted extended shape in solution. As a control oligomer, oligo-NSG (7-NSG) with the same chain length, the same *N*-substituents, and the same terminal structures were synthesized and measured. This oligomer exhibited a much shorter mean length than oligo-NSA, 21 Å (Figure 4h) and a larger distribution, 8 Å. The average distance is too short to consider that the oligomer forms an extended shape. This result suggests that oligo-NSG is more flexible than oligo-NSA and does not persistently form an extended shape in solution. Recently, Hawker and coworkers reported similar DEER measurements of oligo-NSG and an oligomer with alternate NSA/NSG residues and showed that both the oligomers are intrinsically disordered.⁴³ Therefore, we also measured the oligomer with alternate NSA/NSG residues and confirmed that the mean distance (20 Å) and distance distribution (8 Å) is more similar to those of oligo-NSG rather than those of oligo-NSA (Figure S23). These results support the validity of the conclusion from the MD simulations, i.e. oligomers with consecutive NSA residues form an extended shape in water and the shape persistence is higher than oligomers with NSG residues or alternating NSA/NSG residues.

Spectroscopic studies. NMR studies were conducted to evaluate the solution structure of oligo-NSA. Several heteropentamers that are expected to exhibit dispersed proton peaks on NMR spectrum were designed and synthesized to obtain information about spatial proximity of protons from 2D-NMR spectrum. Among those, NSA heteropentamer **8** satisfied the requirement and all the α -protons and N_α protons of the oligomer on ¹H NMR spectrum (Figure S24) were successfully assigned unambiguously for this oligomer using COSY (Figure S25), ¹³C NMR (Figure S26) and HMBC spectra (Figure S27). Although the *N*-substituents differ between oligomer **6** used for crystallographic analysis and oligomer **8** used for NMR analysis, their backbone conformation must closely resemble each other, not to say be identical, because the extended backbone conformation is dictated without the aid of *N*-substituents as described above. The NOESY spectrum of the pentamer **8** was measured to obtain information about spatial proximities among backbone atoms in an oligomer (Figures 5a, S28, and S29). To evaluate backbone conformation, interresidue NOEs among protons on α , β , and N_α positions were analyzed. As a result, first, all amide bonds were confirmed to be in *trans* from interresidue NOEs between protons on an N_α -carbon and the backbone α -proton of the preceding alanine residue (Figure 5a left). Restriction of ϕ of N_α carbon to 180° by the amide bond

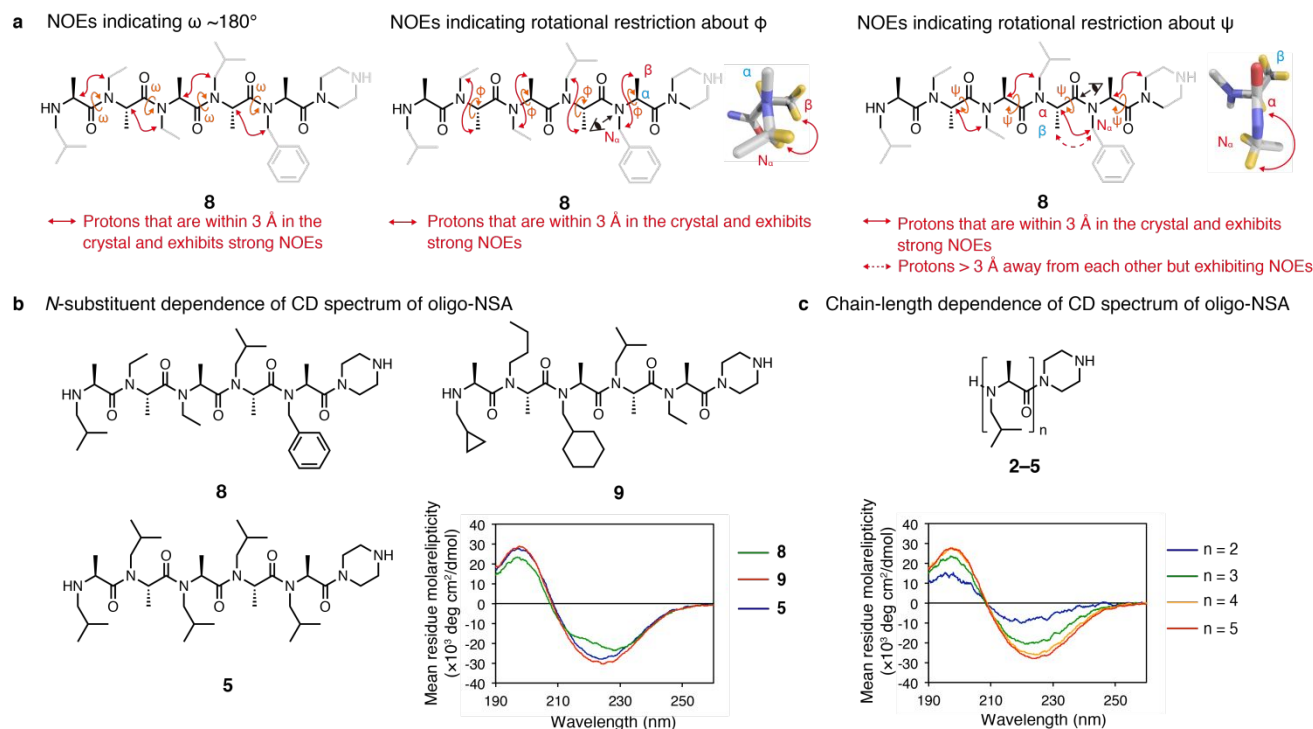


Figure 5. Conformational studies of oligo-NSAs in aqueous solution. (a) A summary of spatial proximity information obtained from a NOESY measurement. Protons with strong NOEs that suggest rotational restrictions about ω (left), ϕ (middle), and ψ (right) are indicated with red solid arrows. Protons with a weak NOE related to ψ (right) are indicated with a red dashed arrow. ¹H NMR spectrum, COSY spectrum, ¹³C NMR spectrum, HMBC spectrum and NOESY spectrum are listed in Figures S24–S29. For the middle and right figures, a part of the crystal structure is shown to visualize the proximities of N_α protons and β protons (middle) or N_α protons and α proton (right). (b) Chemical structures and CD spectra of NSA pentamers **8**, **9**, and **5**. (c) Chemical structures and CD spectra of oligo-NSA **2-5**. The CD spectra were recorded at 25 °C with 100 μ M solution of each oligomer in phosphate buffer (pH 7.2). The Y-axis was normalized to molar ellipticity per residue.

rotations about ϕ angles by pseudo-1,3-allylic strain is expected to result in the intraresidue β and N_α protons being close to each other while intraresidue α and N_α protons are away from each other. The existence of strong NOEs between intraresidue β and N_α protons and absence of NOEs between intraresidue α and N_α protons supports the restricted rotation about ϕ angles around the value observed at the crystal structure (Figure 5a, middle). Similarly, the restriction of bond rotations about ψ angles by pseudo-1,3-allylic strain is expected to result in the N_α protons and α proton of the preceding alanine residue to be close to each other, while N_α protons and β protons of preceding alanine are away from each other. The existence of strong interresidue NOEs between N_α protons and α proton of the preceding alanine residue supports the restricted rotation about ψ angles around the value observed at the crystal structure (Figure 5a, right). The validity of the interpretation of the observed NOEs was ensured with QM calculations of a model NSA dimer where a ϕ or ψ angle was systematically rotated and distances between N_α protons and α or β protons on each optimized structure were measured (Figure S30). Because the β protons of 4th residue exhibited a weak NOE with the N_α protons of 5th residue, despite the fact that those protons are more than 3 Å away from each other in the crystal structure (Figure 5a, right, red dashed lines), some degree of rotation may be allowed for the ψ angle. Together with the absence of NOEs among nonneighboring remote residues, the overall NMR results indicate that the extended conformation of oligo-NSAs seen in the crystal is persistent in aqueous solution. We also measured the NMR spectrum of the

same oligomer in acetonitrile- d_3 and methanol- d_4 to check the solvent dependency of the conformation. In both solvents, almost the same NOEs were observed, indicating that the oligomer forms the same conformation in organic solvents (Figure S31–42). This supports our hypothesis that the conformation of oligo-NSA is dictated by local steric interactions and not dictated by other remote interactions such as hydrophobic interactions or electronic interactions among N -substituents.

We also conducted a CD spectroscopic analysis of oligo-NSA to evaluate the effects of the N -substituents, concentration, solvent and length of the oligomer on conformation of oligo-NSA. First, CD spectra of oligomer **8**, another heteropentamer **9**, and a homopentamer **5** were measured to check the sequence dependency of the backbone conformation. All three oligomers exhibited strong signals and a similar spectral shape with a maximum around at 195 nm and a minimum around at 225 nm (Figure 5b). This result indicates a specific set of backbone dihedral angles is repeated in an oligomer that is independent from N -substituent structures. This is consistent with the highly restricted backbone dihedral angles in the QM calculation. The spectrum of homopentamer **5** did not show concentration dependence of the oligomer, which eliminates the possibility that the ordered structure is realized by aggregation of the oligomer (Figure S43a). The spectral shape did not change in acetonitrile or methanol, which are less polar solvent than water (Figure S43b). This confirms that the conformation is realized by local steric effects on backbone. The spectral shape in aqueous

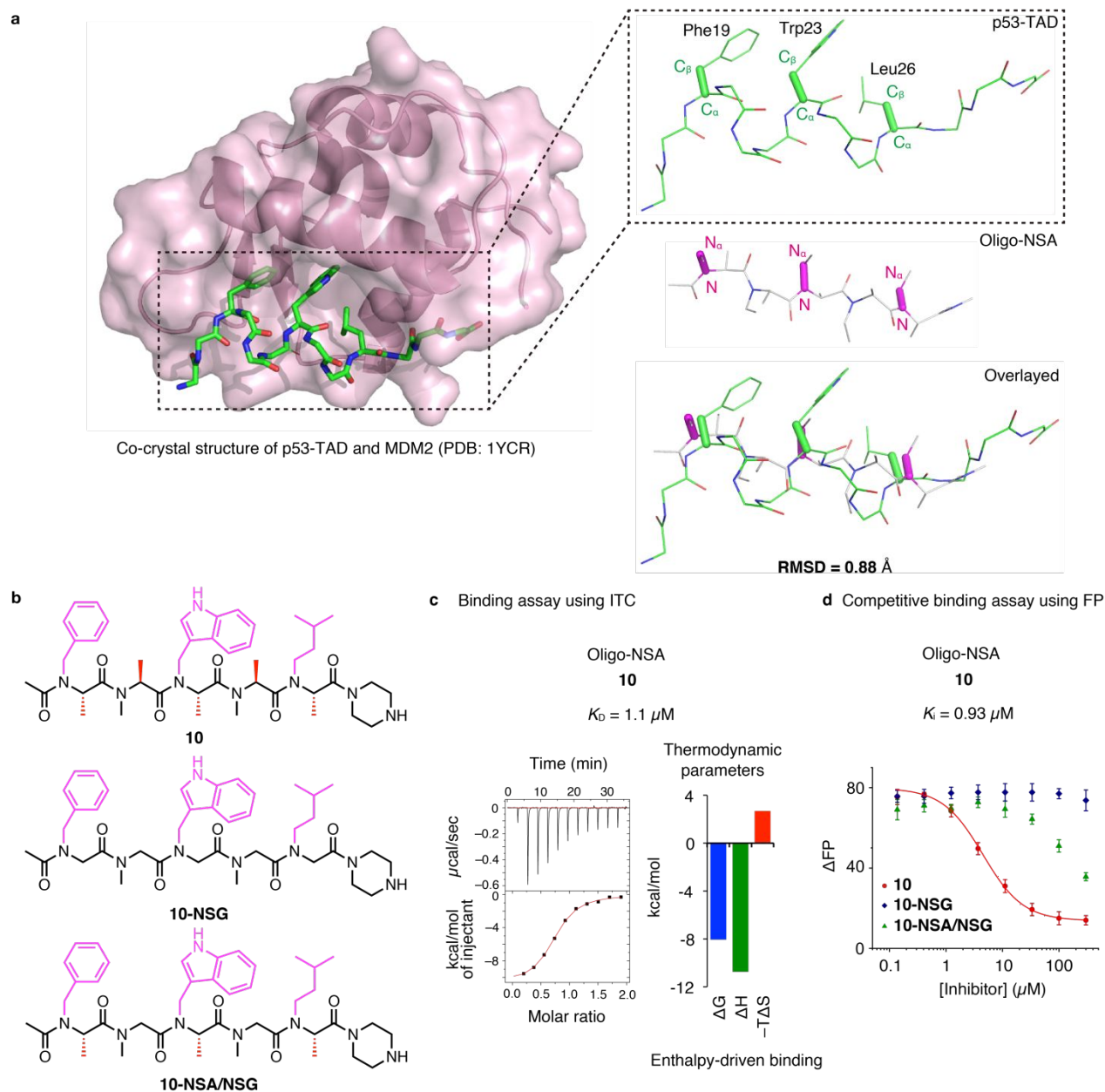


Figure 6. Design and binding assays of MDM2-binding oligo-NSA. (a) (Left) The crystal structure of p53-TAD binding to MDM2 from PDB 1YCR. (Right, top) An enlarged view of p53-TAD in the left figure. The bonds connecting the α carbon (C_α) and β carbon (C_β) of hot-spot residues (Phe19, Trp23 and Leu26) are shown with bold sticks. (Right, middle) The model structure of oligo-NSA pentamer from Figure 2f. For oligo-NSA, the bonds connecting amide nitrogen (N) and N_α carbon (N_α) of the 1st, 3rd, and 5th residues are shown with bold sticks colored in magenta. (Right, bottom) The overlay of the above two structures. The RMSD value for C_α and C_β of hot-spot residues in p53-TAD and N and N_α of 1st, 3rd, and 5th residues of oligo-NSA is described at the bottom. (b) Structures of oligo-NSA (**10**), oligo-NSG (**10-NSG**) and oligomer with alternating NSA/NSG residues (**10-NSA/NSG**) that bears functional *N*-substituents (magenta) corresponding to hot-spot residues of p53-TAD. (c) ITC profiles of interaction between the oligo-NSA (**10**) and MDM2. ITC data with full parameters obtained from the fitting are shown in Figure S43a. (d) Inhibitory curves of **10** (red), **10-NSG** (blue) and **10-NSA/NSG** (green) against the interaction between fluorescently labeled p53-TAD peptide and MDM2 generated from a competitive fluorescence polarization assay. Error bars represent standard deviations of triplicates. The competitive binding data with full parameters obtained from the fitting are shown in Figure S45.

buffer was also insensitive to temperature from 5 °C to 85 °C, which indicates the extended structure is thermally stable (Figure S43c and d). Shorter oligomers, tetramer and trimer, exhibited similar spectra to the pentamers and even dimer exhibited a similar spectral shape, although the intensity was little weaker than in longer oligomers (Figure 5c). This result suggests that an NSA residue is intrinsically restricted in

rotations about backbone dihedral angles and oligomers with consecutive NSA residues uniformly exhibit a constrained conformation composed of repetition of a similar set of backbone dihedral angles, most probably around $(\varphi, \psi) = (-120^\circ, 90^\circ)$, which was found to be the lowest energy point in the QM calculation.

Application of oligo-NSA to biomolecular recognition.

Thus far, we have shown that the rotations about all the three backbone dihedral angles, ϕ , ψ and ω , of oligo-NSA are restricted per-residue basis, which leads to the persistent formation of the extended shape of the oligomer in solution. This rigid structure together with its good water solubility and facile introduction of various *N*-substituents makes oligo-NSA a promising scaffold for displaying multiple functional groups in a well-defined three-dimensional space. Therefore, we hypothesized that oligo-NSA displaying hot spot residues involved in protein-protein interactions in an appropriate order would effectively bind to proteins. To examine this hypothesis, we designed an oligo-NSA that binds to MDM2. MDM2 is recognized by three hot spot residues, Phe19, Trp23 and Leu26, displayed on the transactivation domain of p53 (p53-TAD). When a previously reported crystal structure of p53-TAD binding to MDM2⁶⁵ was overlaid with the model structure of oligo-NSA generated from the QM calculations (Figure 2f), *N*-substituents of every other residue of oligo-NSA were approximately overlapped with the three hot spot residues of p53-TAD (Figure 6a). More specifically, C $_{\alpha}$ and C $_{\beta}$ atoms of the three hot-spot residues of p53-TAD and *N* and N $_{\alpha}$ atoms of the 1st, 3rd, and 5th residues of the model oligo-NSA matched with RMSD value of 0.88 Å. Based on this result, we designed and synthesized oligo-NSA **10** that bears benzyl, indolylmethyl and isopentyl substituents at the 1st, 3rd, and 5th residues (Figure 6b) assuming that the oligo-NSA mimics p53-TAD and binds to MDM2. During the synthesis of the designed oligomer, it was found that the indolylmethyl group was difficult to install using the reductive amination protocol described above. This is probably because an aldehyde with an electron-rich aromatic group like indole directly connected to the carbonyl carbon poorly reacts with the terminal amine of oligo-NSA. Therefore, we recruited reductive amination conditions reported previously where acidic conditions and a dehydrating solvent, trimethyl orthoformate, are used for imine formation.^{66,67} With this reductive amination conditions, indolylmethyl group was successfully installed as *N*-substituents and the designed oligo-NSA was successfully synthesized.

The synthesized ligand was confirmed to bind to MDM2 by isothermal titration calorimetry (ITC). The dissociation constant (K_D) was determined to be 1.1 μ M (Figures 6c and S44a). The binding was enthalpy-driven ($\Delta H = -10.8$ kcal/mol, $-T\Delta S = 2.7$ kcal/mol, and $\Delta G = -8.1$ kcal/mol), suggesting that the interaction is not caused by nonspecific hydrophobic contacts, but realized by specific interactions.

The designed oligo-NSA was confirmed to bind to MDM2 at the same binding site with p53-TAD by a competitive fluorescent polarization assay using a fluorescently labeled p53-TAD peptide. The oligo-NSA **10** competed with the p53-TAD peptide with K_i value of 0.93 μ M (Figures 6d and S45). (As a reference, the binding isotherm of the fluorescently labeled p53-TAD and MDM2 is shown in Figure S46.)

Finally, we examined the importance of the conformationally constrained oligo-NSA backbone for the MDM2 binding because protein ligands based on a rigid scaffold are not necessarily always optimal ligands.⁶⁸ The same set of binding assays and competitive binding assays of control oligomers that completely or partially lose NSA backbones was conducted. Oligo-NSG bearing the same *N*-substituents with the oligo-NSA **10** (**10-NSG**) did not generate substantial amount of heat upon titration on MDM2 suggesting

the binding is much weaker than the corresponding oligo-NSA (**10**) (Figure S44b). In addition, the oligo-NSG did not compete with p53-TAD peptide for MDM2 binding up to 300 μ M (Figure 6d), which further supports the much lower affinity of the oligo-NSG compared to the corresponding oligo-NSA. An oligomer with alternating NSA and NSG residues bearing the same *N*-substituents with the oligo-NSA **10** (**10-NSA/NSG**) also did not generate as much heat as oligo-NSA **10** did as seen in the ITC profile (Figure S44c) and the competitive fluorescence polarization assay showed that the oligomer (**10-NSA/NSG**) binds to MDM2 much less strongly than oligo-NSA **10** (Figure 6d).

These results demonstrated the utility of oligo-NSA as a scaffold for protein binders. Besides, the importance of conformational constraints on peptoid for achieving the efficient protein binding was also demonstrated, at least for the current example. The α -helix mimetic based on the β -strand-like scaffold is reminiscent of the β -hairpin scaffold reported by Robinson and co-workers.⁶⁹ The per-residue conformational control of oligo-NSA realized a smaller α -helix mimic than the β -hairpin-based mimic.

Many preceding reports described the mimicry of α -helical protein-protein interactions using small molecules, e.g. terphenyl and oligobenzamides, and some of these molecules exhibited comparable or even better MDM2-binding affinities than the oligo-NSA **10**. However, the synthetic flexibility of oligo-NSA is its advantageous feature as a molecular scaffold over other molecules. In future, this unique feature will facilitate (1) medicinal chemistry on the lead compound **10** to produce more potent MDM2 inhibitors and (2) rational design of inhibitors of other protein-protein interactions, especially those mediated by α -helices and β -sheets.

CONCLUSIONS

In this study, we achieved efficient synthesis of optically pure oligo-NSA and demonstrated the following three notable features of oligo-NSA: 1) all three backbone dihedral angles, ϕ , ψ and ω , of oligo-NSA are controlled per residue basis irrespective of the structure of *N*-substituents, which leads to the well-defined extended shape of the oligomer, 2) the oligomer exhibits good water solubility, and 3) the efficient submonomer synthetic method allows facile introduction of various functional groups as *N*-substituents. These features make the extended shape of oligo-NSA an attractive scaffold for rational design of protein ligands. The utility of oligo-NSA as a scaffold was clearly demonstrated by the generation of a MDM2 ligand. The backbone mutational study conducted on the MDM2 ligand successfully demonstrated that the introduction of conformational restriction on peptoid is important to realize efficient protein binding. The side-chain independent formation of the well-defined backbone shape allowed the facile generation of protein ligands via the rational approach.

As stated in the introduction, many oligo(*N*-substituted amides) including oligo-NSG have been reported as peptoids. Among the large collection of such peptoids, oligo-NSA is unique for the per-residue program of backbone conformations. This allows oligo-NSA to form a well-defined shape that is well-predictable from the monomer structure and liberate *N*-substituents, or side chains for biomolecular recognitions or other functions.

There are also limitations in the current state of oligo-NSA chemistry. First, although we successfully synthesized oligo-

NSA up to pentamer, the yields were modest or low. Especially, for heteropentamers with polar residues, the yields were very low. In addition, the synthesis involves long coupling reactions. To accelerate further research on oligo-NSA, more efficient and rapid synthetic methods should be developed in future. Second, the shape of oligo-NSA is limited to the extended shape when only L-alanine is used as submonomer. The extended shape can be utilized as a helix mimetic as demonstrated in this study and possibly also as a β -strand mimetic. As protein-protein interaction interfaces consist of a diverse tertiary structure, expansion of the shape diversity is desirable to utilize oligo-NSA as more widely applicable protein capture agents. Introduction of amino acids that prefer different area of the Ramachandran plot is a promising strategy to achieve the goal. Plausible candidates are β -branched amino acids, e.g. valine, and D-alanine. Also, insertion of other conformationally preorganized amino acids, such as L/D-proline, would realize different folded shapes. Third, the oligo-NSA lacks backbone amide hydrogens, which prohibit the backbone to make hydrogen bonds with target proteins. This limitation needs to be backed up by introducing hydrogen bonding donors on *N*-substituents in the current design of oligo-NSA or by introducing other peptoid-type backbone units possessing hydrogen bonding donors, such as aza-peptoids.^{70,71} Resolving these limitations, in future research, would further facilitate the biological applications of oligo-NSA.

In conclusion, the oligo-NSA opens up a new avenue for conformational programs of peptoids and expands the utility of peptoids for biological applications.

ASSOCIATED CONTENT

Supporting Information

The Supporting Information is available free of charge on the ACS Publications website.

Additional figures, and tables and compound characterization data (PDF).

AUTHOR INFORMATION

Corresponding Author

J.M.: jmorimoto@chembio.t.u-tokyo.ac.jp
S.S.: ssando@chembio.t.u-tokyo.ac.jp

Author Contributions

‡These authors contributed equally.

Funding Sources

S.S. acknowledges financial support from CREST (JPMJCR13L4), Japan Science and Technology Agency. J.M. acknowledges financial support from JSPS (JP17K13265 and JP19K15692). D.K. acknowledges financial support from JSPS (JP17K18113) and AMED (JP18fm0208022h). K.T. acknowledges financial support from JSPS (JP16H02420 and JM17H06109) and AMED (JP19am0101094).

Notes

The authors (J. M., Y. F. and S. S.) have filed a patent application (PCT/JP2019/124016).

ACKNOWLEDGMENTS

The computations were performed using Research Center for Computational Science, Okazaki, Japan. We thank Dr. H. Sato Mr. S. Suginome, Dr. S. Kusumoto, Dr. M. Akiyama, and Dr. Okitsu at the University of Tokyo and Dr. H. Sato at Rigaku for the support on X-ray crystallographic analysis. We thank Drs. Y. Goto and H. Suga at the University of Tokyo for the use of a CD spectrometer. The X-ray diffraction data of the crystal was collected using an instrument at Advanced Characterization Nanotechnology Platform of the University of Tokyo, supported by “Nanotechnology Platform” of the Ministry of Education, Culture, Sports, Science and Technology (MEXT), Japan. This work was partly supported by Platform Project for Supporting Drug Discovery and Life Science Research (Basis for Supporting Innovative Drug Discovery and Life Science Research (BINDS)) from AMED (JP18am0101094). This work was partly supported by Nanotechnology Platform Program (Molecule and Material Synthesis) of MEXT, Japan. This work was partly supported by the World-leading Innovative Graduate Study Program for Life Science and Technology, The University of Tokyo, as part of the WISE Program (Doctoral Program for World-leading Innovative & Smart Education), MEXT, Japan.

REFERENCES

- (1) Cheng, R. P.; Gellman, S. H.; Degrado, W. F. β -Peptides: From Structure to Function. *Chem. Rev.* **2001**, *101*, 3219–3232.
- (2) Seebach, D.; Gardiner, J. β -Peptidic Peptidomimetics. *Acc. Chem. Res.* **2008**, *41*, 1366–1375.
- (3) Blasio, D.; Crisma, M. The Longest, Regular Polypeptide 3_{10} Helix at Atomic Resolution. *J. Mol. Biol.* **1990**, *214*, 633–635.
- (4) Le Bailly, B. A. F.; Clayden, J. Dynamic Foldamer Chemistry. *Chem. Commun.* **2016**, *52*, 4852–4863.
- (5) Fischer, L.; Claudon, P.; Pendem, N.; Miclet, E.; Didierjean, C.; Ennifar, E.; Guichard, G. The Canonical Helix of Urea Oligomers at Atomic Resolution: Insights into Folding-Induced Axial Organization. *Angew. Chem. Int. Ed.* **2010**, *49*, 1067–1070.
- (6) Collie, G. W.; Pulka-Ziach, K.; Lombardo, C. M.; Fremaux, J.; Rosu, F.; Decossas, M.; Mauran, L.; Lambert, O.; Gabelica, V.; Mackereth, C. D.; Guichard, G. Shaping Quaternary Assemblies of Water-Soluble Non-Peptide Helical Foldamers by Sequence Manipulation. *Nat. Chem.* **2015**, *7*, 871–878.
- (7) Farmer, P.; Ariëns, E. Speculations on the Design of Nonpeptidic Peptidomimetics. *Trends Pharmacol. Sci.* **1982**, *3*, 362–365.
- (8) Horwell, D. C. Use of the Chemical Structure of Peptides as the Starting Point to Design Nonpeptide Agonists and Antagonists at Peptide Receptors: Examples with Cholecystokinin and Tachykinins. *Bioorg. Med. Chem.* **1996**, *4*, 1573–1576.
- (9) Simon, R. J.; Kania, R. S.; Zuckermann, R. N.; Huebner, V. D.; Jewell, D. A.; Banville, S.; Ng, S.; Wang, L.; Rosenberg, S.; Marlowe, C. K.; Spellmeyer, D. C.; Tan, R.; Frankel, A. D.; Santi, D. V.; Cohen, F. E.; Bartlett, P. A. Peptoids: a Modular Approach to Drug Discovery. *Proc. Natl. Acad. Sci. U. S. A.* **1992**, *89*, 9367–9371.
- (10) Miller, S. M.; Simon, R. J.; Ng, S.; Zuckermann, R. N.; Kerr, J. M.; Moos, W. H. Comparison of the Proteolytic Susceptibilities of Homologous L-Amino Acid, D-Amino Acid, and N-Substituted Glycine Peptide and Peptoid Oligomers. *Drug Dev. Res.* **1995**, *35*, 20–32.

- (11) Yu, P.; Liu, B.; Kodadek, T. A High-Throughput Assay for Assessing the Cell Permeability of Combinatorial Libraries. *Nat. Biotechnol.* **2005**, *23*, 746–751.
- (12) Zuckermann, R. N.; Kerr, J. M.; Kent, S. B. H.; Moos, W. H. Efficient Method for the Preparation of Peptoids [Oligo(N-Substituted Glycines)] by Submonomer Solid-Phase Synthesis. *J. Am. Chem. Soc.* **1992**, *114*, 10646–10647.
- (13) Zuckermann, R. N.; Martin, E. J.; Spellmeyer, D. C.; Stauber, G. B.; Shoemaker, K. R.; Kerr, J. M.; Figliozzi, G. M.; Goff, D. A.; Siani, M. A.; Simon, R. J.; Banville, S. C.; Brown, E. G.; Wang, L.; Richter, L. S.; Moos, W. H. Discovery of Nanomolar Ligands for 7-Transmembrane G-Protein-Coupled Receptors from a Diverse N-(Substituted)glycine Peptoid Library. *J. Med. Chem.* **1994**, *37*, 2678–2685.
- (14) Wu, C. W.; Sanborn, T. J.; Huang, K.; Zuckermann, R. N.; Barron, A. E. Peptoid Oligomers with α -Chiral, Aromatic Side Chains: Sequence Requirements for the Formation of Stable Peptoid Helices. *J. Am. Chem. Soc.* **2001**, *123*, 6778–6784.
- (15) Shah, N. H.; Butterfoss, G. L.; Nguyen, K.; Yoo, B.; Bonneau, R.; Rabenstein, D. L.; Kirshenbaum, K. Oligo(N-aryl glycines): A New Twist on Structured Peptoids. *J. Am. Chem. Soc.* **2008**, *130*, 16622–16632.
- (16) Stringer, J. R.; Crapster, J. A.; Guzei, I. A.; Blackwell, H. E. Extraordinarily Robust Polyproline Type I Peptoid Helices Generated via the Incorporation of α -Chiral Aromatic N-1-Naphthylethyl Side Chains. *J. Am. Chem. Soc.* **2011**, *133*, 15559–15567.
- (17) Gorske, B. C.; Stringer, J. R.; Bastian, B. L.; Fowler, S. A.; Blackwell, H. E. New Strategies for the Design of Folded Peptoids Revealed by a Survey of Noncovalent Interactions in Model Systems. *J. Am. Chem. Soc.* **2009**, *131*, 16555–16567.
- (18) Gorske, B. C.; Mumford, E. M.; Conry, R. R. Tandem Incorporation of Enantiomeric Residues Engenders Discrete Peptoid Structures. *Org. Lett.* **2016**, *18*, 2780–2783.
- (19) Gorske, B. C.; Mumford, E. M.; Gerrity, C. G.; Ko, I. Peptoid Square Helix via Synergistic Control of Backbone Dihedral Angles. *J. Am. Chem. Soc.* **2017**, *139*, 8070–8073.
- (20) Caumes, C.; Roy, O.; Faure, S.; Taillefumier, C. The Click Triazolium Peptoid Side Chain: A Strong Cis-Amide Inducer Enabling Chemical Diversity. *J. Am. Chem. Soc.* **2012**, *134*, 9553–9556.
- (21) Roy, O.; Caumes, C.; Esvan, Y.; Didierjean, C.; Faure, S.; Taillefumier, C. The Tert-Butyl Side Chain: A Powerful Means to Lock Peptoid Amide Bonds in the Cis Conformation. *Org. Lett.* **2013**, *15*, 2246–2249.
- (22) Roy, O.; Dumonteil, G.; Faure, S.; Jouffret, L.; Kriznik, A.; Taillefumier, C. Highly Homogeneous and Robust Polyproline Type I Helices from Peptoids with Non-Aromatic α -Chiral Side Chains. *J. Am. Chem. Soc.* **2017**, *139*, 13533–13540.
- (23) Sanborn, T. J.; Wu, C. W.; Zuckermann, R. N.; Barron, A. E. Extreme Stability of Helices Formed by Water-Soluble Poly-N-Substituted Glycines (Polypeptoids) with α -Chiral Side Chains. *Biopolymers* **2002**, *63*, 12–20.
- (24) Shin, S. B. Y.; Kirshenbaum, K. Conformational Rearrangements by Water-Soluble Peptoid Foldamers. *Org. Lett.* **2007**, *9*, 5003–5006.
- (25) Fuller, A. A.; Yurash, B. A.; Schaumann, E. N.; Seidl, F. J. Self-Association of Water-Soluble Peptoids Comprising (S)-N-1-(Naphthylethyl)glycine Residues. *Org. Lett.* **2013**, *15*, 5118–5121.
- (26) Darapaneni, C. M.; Kaniraj, P. J.; Maayan, G. Water Soluble Hydrophobic Peptoids via a Minor Backbone Modification. *Org. Biomol. Chem.* **2018**, *16*, 1480–1488.
- (27) Hamper, B. C.; Kolodziej, S. A.; Scates, A. M.; Smith, R. G.; Cortez, E. Solid Phase Synthesis of β -Peptoids: N-Substituted β -Aminopropionic Acid Oligomers. *J. Org. Chem.* **1998**, *63*, 708–718.
- (28) Laursen, J. S.; Harris, P.; Fristrup, P.; Olsen, C. A. Triangular Prism-Shaped β -Peptoid Helices as Unique Biomimetic Scaffolds. *Nat. Commun.* **2015**, *6*, 7013.
- (29) Lee, K. J.; Lee, W. S.; Yun, H.; Hyun, Y. J.; Seo, C. D.; Lee, C. W.; Lim, H. S. Oligomers of N-Substituted β^2 -Homoalanines: Peptoids with Backbone Chirality. *Org. Lett.* **2016**, *18*, 3678–3681.
- (30) Morimoto, J.; Fukuda, Y.; Sando, S. Solid-Phase Synthesis of β -Peptoids with Chiral Backbone Substituents Using Reductive Amination. *Org. Lett.* **2017**, *19*, 5912–5915.
- (31) Cheguillaume, A.; Lehardy, F.; Bouget, K.; Baudy-Floc'h, M.; Le Grel, P. Submonomer Solution Synthesis of Hydrazinoazapeptoids, a New Class of Pseudopeptides. *J. Org. Chem.* **1999**, *64*, 2924–2927.
- (32) Shin, I.; Park, K. Solution-Phase Synthesis of Aminoxy Peptoids in the C to N and N to C Directions. *Org. Lett.* **2002**, *4*, 869–872.
- (33) Combs, D. J.; Lokey, R. S. Extended Peptoids: A New Class of Oligomers Based on Aromatic Building Blocks. *Tetrahedron Lett.* **2007**, *48*, 2679–2682.
- (34) Taillefumier, C.; Nielsen, J.; Hjelmggaard, T.; Faure, S.; Staerk, D. Expedient Solution-Phase Synthesis and NMR Studies of Arylopeptoids. *European J. Org. Chem.* **2011**, *2011*, 4121–4132.
- (35) Gao, Y.; Kodadek, T. Synthesis and Screening of Stereochemically Diverse Combinatorial Libraries of Peptide Tertiary Amides. *Chem. Biol.* **2013**, *20*, 360–369.
- (36) Kodadek, T.; McEnaney, P. J. Towards Vast Libraries of Scaffold-Diverse, Conformationally Constrained Oligomers. *Chem. Commun.* **2016**, *52*, 6038–6059.
- (37) Hoffmann, R. W. Allylic 1,3-Strain as a Controlling Factor in Stereoselective Transformations. *Chem. Rev.* **1989**, *89*, 1841–1860.
- (38) Hoffmann, R. W. Flexible Molecules with Defined Shape-Conformational Design. *Angew. Chem. Int. Ed.* **1992**, *31*, 1124–1134.
- (39) Moehle, K.; Hofmann, H. J. Peptides and Peptoids-A Quantum Chemical Structure Comparison. *Biopolymers* **1996**, *38*, 781–790.
- (40) Butterfoss, G. L.; Renfrew, P. D.; Kuhlman, B.; Kirshenbaum, K.; Bonneau, R. A Preliminary Survey of the Peptoid Folding Landscape. *J. Am. Chem. Soc.* **2009**, *131*, 16798–16807.
- (41) Fernández-Llamazares, A. I.; Spengler, J.; Albericio, F. Backbone N-Modified Peptides: How to Meet the Challenge of Secondary Amine Acylation. *Biopolymers* **2015**, *104*, 435–452.
- (42) Pels, K.; Kodadek, T. Solid-Phase Synthesis of Diverse Peptide Tertiary Amides by Reductive Amination. *ACS Comb. Sci.* **2015**, *17*, 152–155.

- (43) Kaminker, R.; Kaminker, I.; Gutekunst, W. R.; Luo, Y.; Lee, S.; Niu, J.; Han, S.; Hawker, C. J. Tuning Conformation and Properties of Peptidomimetic Backbones Through Dual: N/C α -Substitution. *Chem. Commun.* **2018**, *54*, 5237–5240.
- (44) Kaminker, R.; Anastasaki, A.; Gutekunst, W. R.; Luo, Y.; Lee, S.-H.; Hawker, C. J. Tuning of Protease Resistance in Oligopeptides Through N-Alkylation. *Chem. Commun.* **2018**, *54*, 9631–9364.
- (45) Zuckermann, R. N.; Kerr, J. M.; Kent, S. B. H.; Moos, W. H.; Simon, R. J.; Goff, D. A. Synthesis of N-Substituted Oligomers. *US Pat. Number US 5831005* **1998**.
- (46) Virgilio, A. A.; Ellman, J. A. Simultaneous Solid-Phase Synthesis of β -Turn Mimetics Incorporating Side-Chain Functionality. *J. Am. Chem. Soc.* **1994**, *116*, 11580–11581.
- (47) Thern, B.; Rudolph, J.; Jung, G. Total Synthesis of the Nematicidal Cyclododecapeptide Omphalotin A by Using Racemization-Free Triphosgene-Mediated Couplings in the Solid Phase. *Angew. Chem. Int. Ed.* **2002**, *41*, 2307–2309.
- (48) Chatterjee, J.; Laufer, B.; Kessler, H. Synthesis of N-Methylated Cyclic Peptides. *Nat. Protoc.* **2012**, *7*, 432–444.
- (49) Morimoto, J.; Kodadek, T. Synthesis of a Large Library of Macrocyclic Peptides Containing Multiple and Diverse N-Alkylated Residues. *Mol. Biosyst.* **2015**, *11*, 2770–2779.
- (50) Fernández-Llamazares, A. I.; García, J.; Soto-Cerrato, V.; Pérez-Tomás, R.; Spengler, J.; Albericio, F. N-Triethylene Glycol (N-TEG) as a Surrogate for the N-Methyl Group: Application to Sansalvamide A Peptide Analogs. *Chem. Commun.* **2013**, *49*, 6430–6432.
- (51) Fernández-Llamazares, A. I.; García, J.; Adan, J.; Meunier, D.; Mitjans, F.; Spengler, J.; Albericio, F. The Backbone N-(4-Azidobutyl) Linker for the Preparation of Peptide Chimera. *Org. Lett.* **2013**, *15*, 4572–4575.
- (52) Zhang, S.; Prabpai, S.; Kongsaree, P.; Arvidsson, P. I. Poly-N-Methylated α -Peptides: Synthesis and X-Ray Structure Determination of β -Strand Forming Foldamers. *Chem. Commun.* **2006**, 497–499.
- (53) Butterfoss, G. L.; Yoo, B.; Jaworski, J. N.; Chorny, I.; Dill, K. A.; Zuckermann, R. N.; Bonneau, R.; Kirshenbaum, K.; Voelz, V. A. De Novo Structure Prediction and Experimental Characterization of Folded Peptoid Oligomers. *Proc. Natl. Acad. Sci. U. S. A.* **2012**, *109*, 14320–14325.
- (54) Voelz, V. A.; Dill, K. A.; Chorny, I. Peptoid Conformational Free Energy Landscapes from Implicit-Solvent Molecular Simulations in AMBER. *Biopolymers* **2011**, *96*, 639–650.
- (55) Park, S. H.; Szeifer, I. Structural and Dynamical Characteristics of Peptoid Oligomers with Achiral Aliphatic Side Chains Studied by Molecular Dynamics Simulation. *J. Phys. Chem. B* **2011**, *115*, 10967–10975.
- (56) Sui, Q.; Borchardt, D.; Rabenstein, D. L. Kinetics and Equilibria of Cis/Trans Isomerization of Backbone Amide Bonds in Peptoids. *J. Am. Chem. Soc.* **2007**, *129*, 12042–12048.
- (57) Huang, J.; MacKerell, A. D. Force Field Development and Simulations of Intrinsically Disordered Proteins. *Curr. Opin. Struct. Biol.* **2018**, *48*, 40–48.
- (58) Mirijanian, D. T.; Mannige, R. V.; Zuckermann, R. N.; Whitelam, S. Development and Use of an Atomistic CHARMM-based Forcefield for Peptoid Simulation. *J. Comput. Chem.* **2014**, *35*, 360–370.
- (59) Prakash, A.; Baer, M. D.; Mundy, C. J.; Pfaendtner, J. Peptoid Backbone Flexibility Dictates Its Interaction with Water and Surfaces: A Molecular Dynamics Investigation. *Biomacromolecules* **2018**, *19*, 1006–1015.
- (60) Milov, A. D.; Ponomarev, A. B.; Tsvetkov, Y. D. Electron-electron Double Resonance in Electron Spin Echo: Model Biradical Systems and the Sensitized Photolysis of Decalin. *Chem. Phys. Lett.* **1984**, *110*, 67–72.
- (61) Pannier, M.; Veit, S.; Godt, A.; Jeschke, G.; Spiess, H. W. Dead-Time Free Measurement of Dipole–Dipole Interactions between Electron Spins. *J. Magn. Reson.* **2000**, *142*, 331–340.
- (62) Tsvetkov, Y. D.; Grishin, Y. A. Techniques for EPR Spectroscopy of Pulsed Electron Double Resonance (PELDOR): A Review. *Instruments Exp. Tech.* **2009**, *52*, 615–636.
- (63) Jeschke, G. DEER Distance Measurements on Proteins. *Annu. Rev. Phys. Chem.* **2012**, *63*, 419–446.
- (64) Jeschke, G.; Sajid, M.; Schulte, M.; Ramezani, N.; Volkov, A.; Zimmermann, H.; Godt, A. Flexibility of Shape-persistent Molecular Building Blocks Composed of p-Phenylene and Ethynylene Units. *J. Am. Chem. Soc.* **2010**, *132*, 10107–10117.
- (65) Kussie, P. H.; Gorina, S.; Marechal, V.; Elenbaas, B.; Moreau, J.; Levine, A. J.; Pavletich, N. P. Structure of the MDM2 Oncoprotein Bound to the p53 Tumor Suppressor Transactivation Domain. *Science* **1996**, *274*, 948–953.
- (66) Look, G. C.; Murphy, M. M.; Campbell, D. A.; Gallop, M. A. Trimethylorthoformate: A Mild and Effective Dehydrating Reagent for Solution and Solid Phase Imine Formation. *Tetrahedron Lett.* **1995**, *36*, 2937–2940.
- (67) Iera, J. A.; Jenkins, L. M. M.; Kajiyama, H.; Kopp, J. B.; Appella, D. H. Solid-phase Synthesis and Screening of N-Acylated Polyamine (NAPA) Combinatorial Libraries for Protein Binding. *Bioorg. Med. Chem. Lett.* **2010**, *20*, 6500–6503.
- (68) Hara, T.; Durell, S. R.; Myers, M. C.; Appella, D. H. Probing the Structural Requirements of Peptoids That Inhibit HDM2–p53 Interactions. *J. Am. Chem. Soc.* **2006**, *128*, 1995–2004.
- (69) Fasan, R.; Dias, R. L. A.; Moehle, K.; Zerbe, O.; Vrijbloed, J. W.; Obrecht, D.; Robinson, J. A. Using a β -Hairpin to Mimic an α -Helix: Cyclic Peptidomimetic Inhibitors of the p53–HDM2 Protein–Protein Interaction. *Angew. Chem. Int. Ed.* **2004**, *43*, 2109–2112s.
- (70) Sarma, B. K.; Yousufuddin, M.; Kodadek, T. Acyl Hydrazides as Peptoid Sub-Monomers. *Chem. Commun.* **2011**, *47*, 10590–10592.
- (71) Sarma, B. K.; Kodadek, T. Submonomer Synthesis of a Hybrid Peptoid – Azapeptoid Library. *ACS Comb. Sci.* **2012**, *14*, 558–564.

1
2
3
4
5
6
7
8
9
10
11
12
13
14
15
16
17
18
19
20
21
22
23
24
25
26
27
28
29
30
31
32
33
34
35
36
37
38
39
40
41
42
43
44
45
46
47
48
49
50
51
52
53
54
55
56
57
58
59
60

